Anisotropic structure analysis for cobalt oxides on α-Al_2O_3 (0001) by polarized total-reflection fluorescence extended X-ray absorption fine structure

M. Shirai, K. Asakura and Y. Iwasawa *

Department of Chemistry, Faculty of Science, The University of Tokyo, 7-3-1, Hongo, Bunkyo-ku, Tokyo, Japan

Received 24 February 1992; accepted 23 May 1992

Anisotropic structure analyses for $[CoO_x]/\alpha$-Al_2O_3 (0001) and $[Co_3O_4]_n/\alpha$-Al_2O_3 (0001) which were derived from $Co_2(CO)_8/\alpha$-Al_2O_3 (0001) were performed by a polarized total-reflection fluorescence extended X-ray absorption fine structure (EXAFS) technique. Both s- and p-polarized EXAFS data revealed that the cobalt atoms of $[CoO_x]$ were located on three-fold hollow sites of α-Al_2O_3 (0001) in a monomer form and that a thin spinel structure $[Co_3O_4]$ grew with the (001) plane parallel to α-Al_2O_3 (0001).

Keywords: Polarized total-reflection fluorescence EXAFS; cobalt oxides on α-Al_2O_3 (0001); anisotropic structure analysis; oxidation catalyst model

1. Introduction

Anisotropic environments of solid surfaces can induce anisotropic/asymmetric growth of surface materials which provide unique catalytic properties. Anisotropic characterization of active structures at surfaces is, therefore, necessary to design new efficient structures/phases with a particular orientation/plane. Active metal/metal oxide sites are usually highly dispersed on inorganic oxide surfaces and this situation has made structural analysis difficult. Among recent physical techniques, EXAFS (extended X-ray absorption fine structure) belongs to the most useful techniques to provide direct information on the structures of this kind of materials [1,2].

We have reported by conventional EXAFS that three atomic layers of Co_3O_4 spinel with the (110) plane on γ-Al_2O_3 powder and one atomic TiO_2 layer with the anatase (110) plane on SiO_2 powder are formed when they are prepared by

* To whom correspondence should be addressed.

the surface reaction of OH groups and organometallic compounds, followed by oxidation [3–7]. However, conventional EXAFS analysis for powder samples shows only averaged local structures over all directions around a particular element, where definite conclusions about asymmetric or anisotropic structures of active sites on support surfaces cannot be obtained.

On the other hand, by using single crystals as supports and polarized EXAFS which shows the dependence of the K-edge EXAFS amplitude on $\cos^2 \theta_{ij}$ as shown in eqs. (1) and (2), one can carry out the anisotropic surface structure analysis.

$$\chi(k) = -3 \sum_i \sum_j \cos^2 \theta_{ij} A_i^*(k) \sin[2kr_i + \phi_i(k)], \tag{1}$$

$$A_i^*(k) = F_i(k) \exp(-2\sigma_i^2 k^2) \exp[-2r_i/\lambda_i(k)]/kr_i^2, \tag{2}$$

where k is the photoelectron wave vector, and $F_i(k)$, $\lambda_i(k)$, ϕ_i, and σ_i represent the amplitude function, the mean free path, the phase shift and the Debye–Waller factor of the ith atom respectively, and θ_{ij} is the angle between the electronic field vector of the incident X-ray and the bond vector r_{ij} [8–12]. In general, the ratio of surface signal to bulk signal (S/B) is low, which makes it difficult to analyze the EXAFS spectra of single crystal samples [13,14].

In this study, we have adopted a total-reflection fluorescence method to overcome this problem. We report for the first time the anisotropic structure analysis of two kinds of cobalt oxides, $[CoO_x]$ and $[Co_3O_4]_n$, on α-Al_2O_3 (0001) which are regarded as models for Al_2O_3-supported Co oxide catalysts. In fact, $Co_2(CO)_8$-derived Co_3O_4 species/α-Al_2O_3 powder showed a remarkably high activity for CO oxidation with O_2 [15].

2. Experimental

The samples were prepared as follows:

$$Co_2(CO)_8 \xrightarrow[313\ K]{\alpha\text{-}Al_2O_3\ (0001)} \xrightarrow[300\ K]{O_2}$$

$$\underset{(A)}{[CoO_x]/\alpha\text{-}Al_2O_3\ (0001)} \xrightarrow[873\ K]{O_2} \underset{(B)}{[Co_3O_4]_n/\alpha\text{-}Al_2O_3\ (0001)}.$$

$Co_2(CO)_8$ vapor was deposited on α-Al_2O_3 (0001) (Kyocera Inc.) for 2 h at room temperature, followed by evacuation at 313 K under vacuum to remote excess Co carbonyls. O_2 (1.7 kPa) was introduced at 300 K for 5 h to form sample A. Then, sample A was oxidized in air at 873 K for 1 h to form sample B.

The atomic ratio of Co atom to surface oxygen atom on α-Al_2O_3 (0001) (Co/O) was estimated by XPS using Co oxide/α-Al_2O_3 (0001) with a known amount of Co atoms as a reference sample.

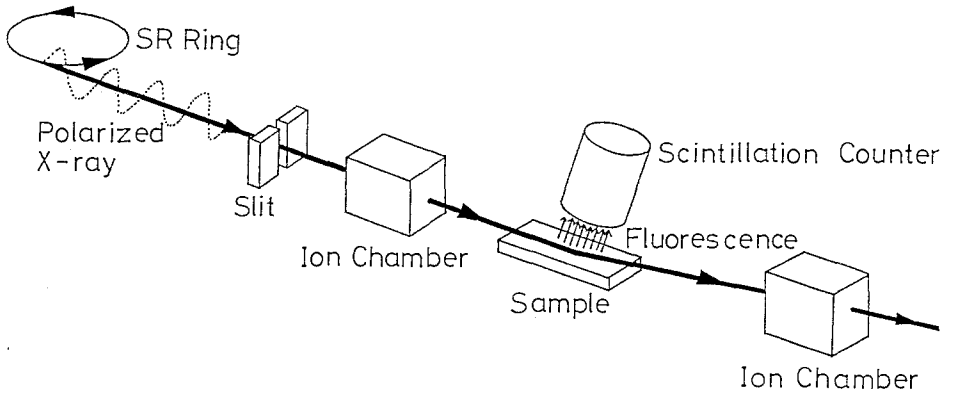

Fig. 1. A schematic diagram of polarized total-reflection fluorescence EXAFS.

Polarized total-reflection fluorescence EXAFS spectra were measured by the EXAFS facilities illustrated in fig. 1 which are installed at BL-14A of Photon Factory in the National Laboratory for High Energy Physics (KEK-PF) [16] (Proposal No. 89-146). A four-axis goniometer equipped at BL-14A was used to set the sample at a particular orientation against the polarization direction of synchrotron and at a total reflection angle. The beam size was 0.1 mm ∅, which does not irradiate to other parts than the sample. The angles between crystal face and polarization direction were set at 90° and 0°. The incident X-ray was monitored by an ion chamber filled with N_2. The fluorescence was detected by a scintillation counter. Fe foil was used as a filter for elastic scattering from the sample. The position of the NaI scintillation counter was adjusted to remove X-ray Bragg-diffraction.

The effective coordination number (N^*) was calculated based on the angle θ_{ij} by

$$N_i^* = 3 \sum_i \sum_j \cos^2 \theta_{ij}. \tag{3}$$

3. Results and discussion

The Fourier transforms of s-polarized and p-polarized total-reflection fluorescence EXAFS spectra of sample A are shown in figs. 2a and 2b, respectively. One peak between 0.1 and 0.2 nm was obtained in both Fourier transforms. Taking into account the bond distance, the peak is assigned to the Co–O bond. No peak is ascribed to Co–Co, suggesting the distribution of Co as a monomer. The Co–Al peak was never observed either. Curve-fitting analysis revealed that the Co–O bond lengths determined by both polarizations are the same, 0.208 nm, with effective coordination numbers of Co–O of 3.3 and 3.9 for 0° and 90°

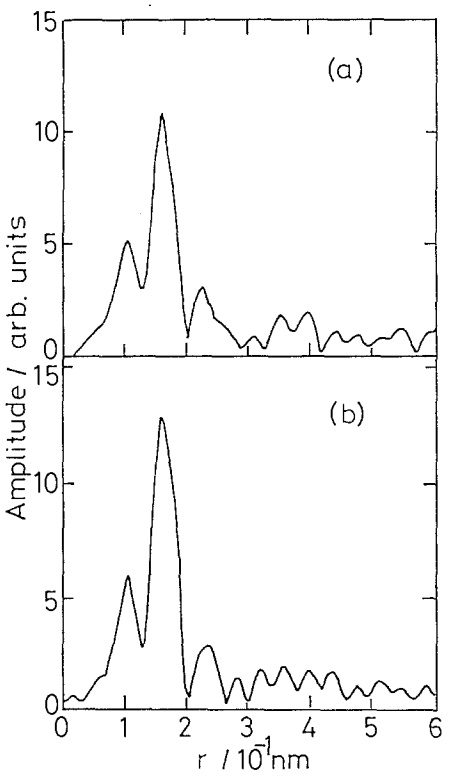

Fig. 2. Fourier transforms for $[CoO_x]/\alpha\text{-}Al_2O_3$ (0001); (a) 0° and (b) 90° polarization.

polarization, respectively (table 1). The ratio of the two effective coordination numbers was 1.2.

The $\alpha\text{-}Al_2O_3$ (0001) surface is illustrated in fig. 3, where an Al atom is surrounded by six oxygen atoms [17]. Assuming the ideal surface structure with O–O distance of 0.275 nm and using the Co–O bond length of 0.208 nm determined by the EXAFS analysis, we calculated the effective coordination number N^* of the Co–O bond based on the three typical structures, "atop", "two-fold bridge site" and "three-fold hollow site" on $\alpha\text{-}Al_2O_3$ (0001) as shown in fig. 3. The N^* values and their ratios calculated from the models and

Table 1
Experimental results and model calculations of the effective coordination number (N^*) for sample A

Polarization	Exp.	On-top	Bridge	Three-fold
0°	3.3 [a]	0	1.3	2.6
90°	3.9 [a]	3	3.3	3.7
ratio (90°/0°)	1.2	∞	2.6	1.4

[a] ±0.7.

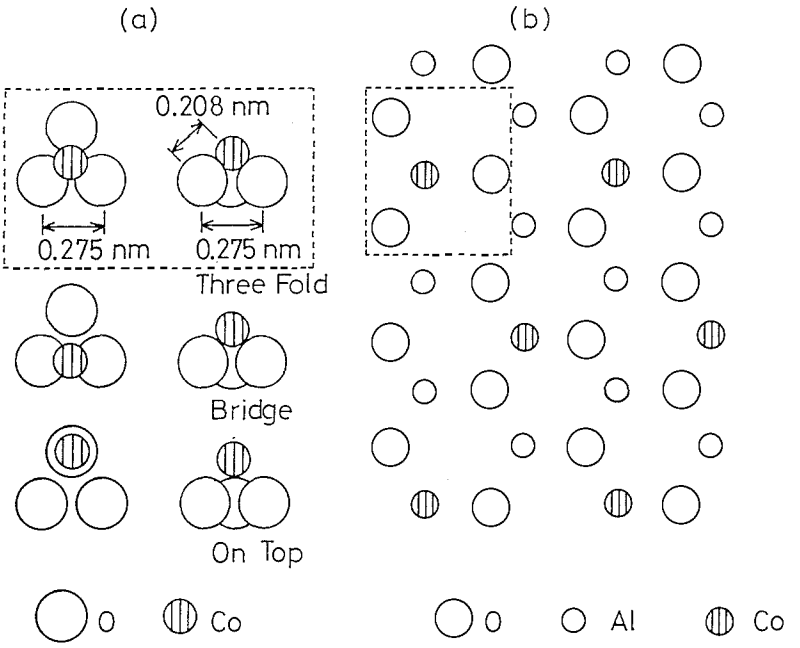

Fig. 3. (a) Models for Co atoms on three sites of α-Al_2O_3 (0001), (b) proposed structure for $[CoO_x]/\alpha$-Al_2O_3 (0001).

obtained by s- and p-polarized total-reflection fluorescence EXAFS analyses are shown in table 1. The experimental values are in agreement with the values of the three-fold hollow site model only. The ratio $N^*(90°)/N^*(0°)$ is well reproduced by the three-fold hollow site model, not by others.

The Co quantity in sample A was determined to be one third of the amount of surface oxygen atoms at α-Al_2O_3 (0001) by XPS. α-Al_2O_3 (0001) consists of a hexagonal stack of O and Al atoms as shown in fig. 3. As the Co–Al bond was not observed, as mentioned above, the Co atoms should be located on the three-fold hollow sites without on-site and adjacent Al atoms (fig. 3). This distribution agrees well with the amount of Co atoms.

The EXAFS Fourier transforms for sample B and the Co_3O_4 bulk are shown in fig. 4. Fourier transforms of both s- and p-polarized EXAFS spectra, have the peaks at similar positions to those for Co_3O_4 in fig. 4. The EXAFS analysis in table 2 confirmed from almost the same bond lengths that sample B takes the spinel structure. The first fourth peaks in fig. 4 are assigned to Co–O, Co(oct)–Co(oct) (oct: octahedral), Co(tet)–Co(oct) and Co(tet)–Co(tet) (tet: tetrahedral), and Co(oct)–Co(oct).

However, there was a difference between the peak intensities in fig. 4 for the analyses parallel and normal to the surface, indicating an asymmetric crystal growth of $[Co_3O_4]_n$ on α-Al_2O_3 (0001). The curve-fitting analysis in table 2 shows that the N^* of the fourth shell decreased to half values as compared to

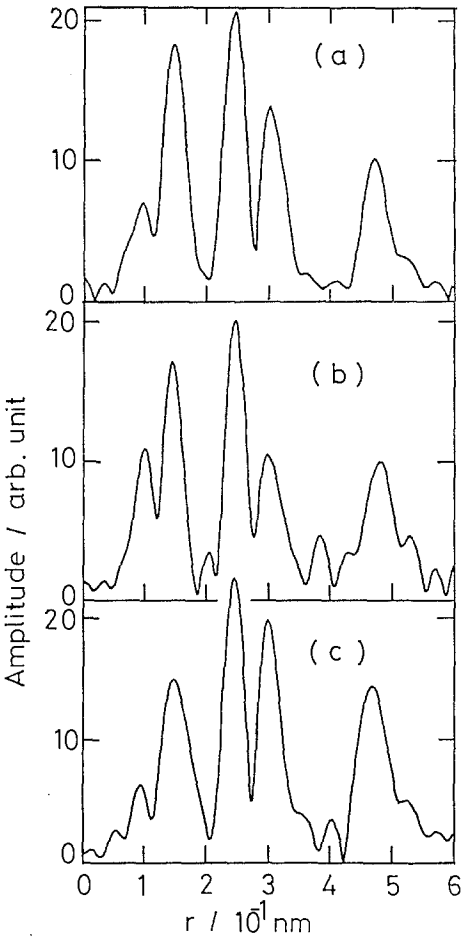

Fig. 4. Fourier transforms of (a) 0° and (b) 90° polarization EXAFS data for $[Co_3O_4]_n$ / α-Al_2O_3 (0001), and Fourier transform for the Co_3O_4 bulk (c).

that for the Co_3O_4 bulk. It means that the size of $[Co_3O_4]_n$ on α-Al_2O_3 (0001) is about 0.9 nm in dimension parallel to the surface, which corresponds to a unit structure of Co_3O_4 spinel. The N^* of the third shell in the Fourier transform of the 90° polarization EXAFS data decreased to 76% of that in the 0° polarization EXAFS Fourier transform.

The ratios of N^* in the second and third Co–Co peaks for both polarizations were calculated for Co_3O_4 (001), (110), and (111) planes which were assumed to grow on α-Al_2O_3 (0001). The expected N^* ratios were plotted for the different numbers of layers in fig. 5, where one-unit structure of the spinel is regarded to consist in eight atomic layers. When seven layers of the (001) plane were considered, the calculated $N^*(90°)/N^*(0°)$ well reproduced the experimental result as shown in fig. 5. All other cases never fitted the observed data.

Table 2
Polarized total-reflection fluorescene EXAFS analyses for sample B (r and σ in nm) [a]

Polarization	Co–O			Co–Co		
	N^*	r	σ	N^*	r	σ
0°	4.2	0.194	0.0036	6.9	0.286	0.0074
90°	5.2	0.192	0.0071	6.0	0.285	0.0074
	Co–Co			Co–Co		
	N^*	r	σ	N^*	r	σ
0°	9.3	0.342	0.0077	3.1	0.496	0.0048
90°	7.1	0.340	0.0077	2.7	0.497	0.0041

[a] For Co–O, N^*: ±0.6, r: ±0.002 nm. For Co–Co, N^*: ±0.1–0.3, r: ±0.001–0.002 nm. For the analysis of Co_3O_4 spinel, Co–O (r = 0.195 nm, N = 5.4), Co–Co (0.286, 6.0), Co–Co (0.338, 9.3), and Co–Co (0.495, 6.0).

Two closest-pack planes (001) and (110) of the spinel crystal should have similar surface energies, but the preferential growth of the (001) plane was observed. This may be due to a large repulsion of the surface oxygen atoms of α-Al_2O_3 (0001) against the first-layer oxygen of the (110) face of the Co_3O_4 spinel crystal, whereas the steric difficulty of stacking can be avoided by the arrangement of the (001) plane where Co atoms may be located on on-top sites

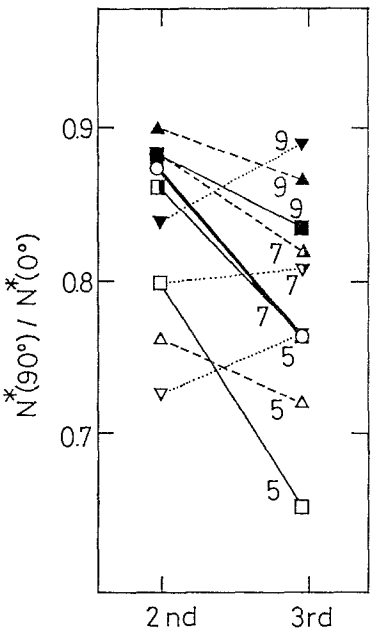

Fig. 5. The ratio of effective coordination number (90°/0° polarization) (○) observed; (□) five (001) layers. (◨) seven layers, (■) nine layers; (△) five (110) layers, (◭) seven layers, (▲) nine layers; (▽) five (111) layers, (▿) seven layers, (▼) nine layers.

at the α-Al_2O_3 (0001) surface. A detailed discussion on this point will be given in a separate paper.

Acknowledgement

We thank Professor M. Nomura (KEK-PF) for helpful discussions and suggestions. This work has been performed under the approval of the Photon Factory Program Advisory Committee (Proposal No. 89-146).

References

[1] J.C.J. Bart and G. Vlaic, Adv. Catal. 35 (1987) 1.
[2] Y. Iwasawa, Adv. Catal. 35 (1987) 87.
[3] Y. Iwasawa, M. Yamada, Y. Sato and H. Kuroda, J. Mol. Catal. 23 (1984) 95.
[4] M. Yamada and Y. Iwasawa, Nippon Kagaku Kaishi (1984) 1042.
[5] K. Asakura, T. Shido and Y. Iwasawa, Shokubai 29 (1987) 166.
[6] K. Asakura and Y. Iwasawa, J. Phys. Chem. 93 (1989) 4231.
[7] K. Asakura and Y. Iwasawa, J. Phys. Chem., in press.
[8] P.A. Lee, Phys. Rev. B13 (1976) 5261.
[9] G. Martens, P. Rabe, N. Schwentner and A. Werner, Phys. Rev. B17 (1978) 1481.
[10] E.A. Stern, Phys. Rev. B10 (1974) 3027.
[11] C.H. Ashley and S. Doniach, Phys. Rev. B11 (1975) 1279.
[12] P.A. Lee and J.B. Pendry, Phys. Rev. B11 (1975) 2795.
[13] L.R. Share, W.R. Heineman and R.C. Elder, Chem. Rev. 90 (1990) 705.
[14] R. Frahm, T.W. Barbee Jr. and W. Warburtron, Phys. Rev. B44 (1991) 2823.
[15] M. Shirai and Y. Iwasawa, unpublished.
[16] Y. Sato and Iitaka, Rev. Sci. Instr. 60 (1989) 2390.
[17] R.W.G. Wryckoff, *Crystal Structure*, 2nd Ed. (Interscience, New York, 1964).